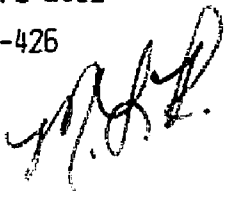


51  
6/15/89

PREPARED FOR THE U.S. DEPARTMENT OF ENERGY,  
UNDER CONTRACT DE-AC02-76-CHO-3073

PPPL-2612  
UC-426

PPPL-2612



(2)

MEASUREMENT OF THE POLOIDAL MAGNETIC FIELD IN THE  
PBX-M TOKAMAK USING THE MOTIONAL STARK EFFECT

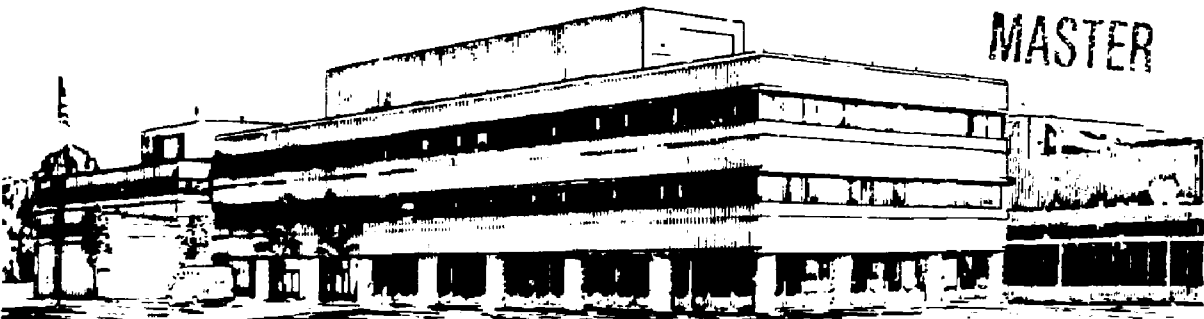
BY

F.M. LEVINTON, R.J. FONCK, G.M. GAMMEL, R. KAITA,  
H.W. KUGEL, E.T. POWELL, AND D.W. ROBERTS

MAY 1989

PRINCETON  
PLASMA PHYSICS  
LABORATORY

MASTER



PRINCETON UNIVERSITY, PRINCETON, NEW JERSEY

NOTICE

Available from:

National Technical Information Service  
U.S. Department of Commerce  
5285 Port Royal Road  
Springfield, Virginia 22161  
703-487-4650

Use the following price codes when ordering:

Price: Printed Copy A03  
Microfiche A01

Measurement of the Poloidal Magnetic Field in the  
PBX-M Tokamak using the Motional Stark Effect

F. M. Levinton

*JAYCOR, Plasma Technology Division, 3547 Voyager Street,*

*Torrance, California 90503*

and

R. J. Fonck, G. M. Gammel, R. Kaita, H. W. Kugel,

E. T. Powell, and D. W. Roberts

*Princeton Plasma Physics Laboratory, Princeton, New Jersey 08543*

**Abstract**

Polarimetry measurements of the Doppler-shifted  $H_{\alpha}$  emission from a hydrogen neutral beam on the PBX-M tokamak have been employed in a novel technique for obtaining  $q(0)$  and poloidal magnetic field profiles. The electric field from the beam particle motion across the magnetic field ( $\mathbf{E} = \mathbf{V}_{\text{beam}} \times \mathbf{B}$ ) causes a wavelength splitting of several angstroms, and polarization of the emitted radiation (Stark effect). Viewed transverse to the fields, the emission is linearly polarized with the angle of polarization related to the direction of the magnetic field.

**DISCLAIMER**

This report was prepared as an account of work sponsored by an agency of the United States Government. Neither the United States Government nor any agency thereof, nor any of their employees, makes any warranty, express or implied, or assumes any legal liability or responsibility for the accuracy, completeness, or usefulness of any information, apparatus, product, or process disclosed, or represents that its use would not infringe privately owned rights. Reference herein to any specific commercial product, process, or service by trade name, trademark, manufacturer, or otherwise does not necessarily constitute or imply its endorsement, recommendation, or favoring by the United States Government or any agency thereof. The views and opinions of authors expressed herein do not necessarily state or reflect those of the United States Government or any agency thereof.

td

The current density profile has played an important role for many years in the theoretical modeling of plasma stability and confinement. Current-driven instabilities have been observed or theorized under various conditions and may be an essential ingredient in plasma confinement and transport. To understand the effects of the current density profile, credible techniques for the measurement of the poloidal field distribution applicable to the present generation of fusion devices are essential. To date, most techniques attempted have suffered from one of several problems. Frequently, the measurement is line-integrated, which requires a numerical inversion process to obtain spatial information.<sup>1,2</sup> This introduces some uncertainty, particularly for non-circular plasma shapes. Neutral beam techniques have shown good spatial resolution, but so far have suffered from beam attenuation for densities above  $\sim 1 \times 10^{13} \text{ cm}^{-3}$ .<sup>3,4</sup>

In this Letter we report the first measurements of the central rotational transform,  $q(0)$ , using the motional Stark effect (MSE) to polarize the spectral emission from a 55 keV neutral hydrogen beam. One of the principal advantages of this technique is that it can provide a local ( $\sim 1 - 2 \text{ cm}$  resolution) measurement of the pitch angle,  $\gamma_p(r) = \tan^{-1}(\frac{B_T(r)}{B_p(r)})$ , where  $B_T$  is the toroidal magnetic field, and  $B_p$  is the poloidal field in the midplane. The pitch angle is related to the safety factor,  $q(r) = r R \tan(\gamma_p(r))$ . The safety factor on the magnetic axis ( $B_p = 0$ ), for a circular plasma, is  $q_{cyl} = 1 R(\frac{d \tan(\gamma_p)}{dr})_{r=0}$ . Another important feature of this method is that beam attenuation is minimal for a hydrogen beam of  $\sim 80 \text{ keV}$  at the operating densities of present-day tokamaks and, hence, this approach extrapolates favorably for use at higher densities and/or in larger machines.

As a neutral beam propagates through a plasma, collisions of the beam particles with the background ions and electrons will excite beam atoms, leading to emission

of radiation. In addition, the motional Stark effect,<sup>3</sup> which arises from the electric field induced in the atom's rest frame due to the motion across the magnetic field ( $\mathbf{E} = \mathbf{V}_{\text{beam}} \times \mathbf{B}$ ), causes both a wavelength splitting of several angstroms, and strong polarization of the emitted radiation. The  $\Delta m = 0$  transitions, or  $\pi$  lines, are linearly polarized parallel to the electric field and the  $\Delta m = \pm 1$  transitions,  $\sigma$  lines, are linearly polarized perpendicular to the electric field, in other words, parallel to the magnetic field when viewed transverse to the field. However, in contrast to the Zeeman effect, the emission is unpolarized when viewed parallel to the field direction. The use of hydrogen has the unique characteristic that the Stark effect is linear with the electric field, producing a large spectral shift. For a magnetic field of 1.3 T and a beam energy of 55 keV, which are typical parameters for the Princeton Beta Experiment (PBX-M) tokamak,<sup>6</sup> the electric field on the atom is  $\sim 40$  kV/cm. The average spectral shift of the  $\pi$  lines for this field is  $\sim 4$  Å. The spectral shift due to the Zeeman effect under these conditions is much less than the Stark shift. This has no effect on the direction of the linearly polarized plane wave. It can change the polarization fraction, but only by a few percent, so this effect can be ignored. The Stark effect pattern of the Balmer-alpha ( $H_\alpha$ ) lines showing the relative line intensities and polarization from Ref. 5, along with a measurement of the polarization fraction profile is shown in Fig. 1. Each data point is a time average of 40 msec from a single PBX-M discharge. Also shown is a numerically computed fractional polarization profile based on the convolution of the Stark shift and filter profile.

The experimental apparatus for these measurements on PBX-M consists of a highly collimated ( $\sim 0.5^\circ$ ) diagnostic neutral hydrogen beam.<sup>7</sup> The energy can be varied from 40-80 keV with a maximum injected power of  $\sim 40$  kW in the full energy

component. The beam power and energy for all the data shown here is 10 kW and 55 keV, respectively. The beam has a cross section of 5 cm vertically and 1.5 cm in the horizontal direction. The injection angle can be varied to change the radial intersection of the viewing cone with the beam, as shown in Fig. 2. The beam angle with respect to the optic axis of the instrumentation is typically 30-40 degrees. A lens mounted on the machine, normal to the magnetic field components, collects the light from the torus. A second lens collimates it through the two photo-elastic modulators, the polarizer, and the interference filter before it is focused onto a photomultiplier tube (PMT). The signal output from the PMT is amplified before going into a lock-in amplifier or waveform digitizer for later analysis. The interference filter is designed to have peak transmission at 6630 Å and a spectral width of 4 Å. The width is chosen to transmit only the  $\sigma$  lines from the  $H_{\alpha}$  spectra in order to maximize the polarization fraction. The filter can be tuned to different wavelengths by tilting it, which shifts the passband towards the blue. This is necessary for maximizing the signal and compensating for different Doppler shifts when the beam angle is changed, as during a radial scan.

The polarimeter design uses a photoelastic modulator (PEM)<sup>9,9</sup> which has a large etendue and very good sensitivity to small variations in the polarization angle. A PEM consists of a birefringent crystal such as quartz with a piezoelectric transducer coupled to the crystal and driven at its resonant frequency ( $\leq 50$  kHz). Due to the birefringence of the crystal, the transducer causes a time-varying phase shift of the electric field between the  $x$  and  $y$  directions through the crystal. This results in a rotation of the input polarized light. In general, with incident linearly polarized light at an angle  $\gamma$ , a PEM at an angle  $\alpha$  and a polarizer analyzer at an angle  $\theta$ , the

transmitted intensity is

$$I = \frac{J_0}{2} [1 - \cos 2(\gamma - \alpha) \cos 2(\theta - \alpha) - \sin 2(\gamma - \alpha) \sin 2(\theta - \alpha) \cos(A_0 \cos \Omega t)], \quad (1)$$

where the following Bessel series expansion can be used for

$$\begin{aligned} \cos(A_0 \cos(\Omega t)) &= J_0(A_0) - 2J_2(A_0) \cos(2\Omega t) \\ &\quad - 2J_4(A_0) \cos(4\Omega t) - \dots \end{aligned} \quad (2)$$

with  $A_0$  the phase shift amplitude, and  $\Omega$  the resonant frequency of the PEM. The phase shift amplitude,  $A_0$ , is adjusted to the maximum of the  $J_2$  Bessel function, so as to maximize the  $\cos(2\Omega t)$  term. This term is optimized because there is no modulation of the  $J_0$  term, so it can be ignored, and the modulation frequency of  $J_4$  and higher terms is too high for the amplifier. The  $J_2$  term has a convenient modulation frequency between 50 - 100 kHz.

With the appropriate choice of parameters, the modulation amplitude can be proportional to the sine or cosine of the angle of polarization of the incident light. With two PEM's at slightly different frequencies both the sine and cosine can be measured simultaneously using synchronous detection techniques. If the corresponding values for  $\alpha$  in Eq.(1) are  $0^\circ$ , and  $45^\circ$ , and  $\theta = -22.5^\circ$  then

$$I \propto (\sin(2\gamma) \cos(2\Omega_2 t) - \cos(2\gamma) \cos(2\Omega_1 t) - \dots) \quad (3)$$

The angle of the linearly polarized light equals the ratio of the signal amplitudes at the two PEM frequencies,  $\tan(2\gamma) = I(2\Omega_2) / I(2\Omega_1)$ . The two amplitudes,  $I(2\Omega_2)$  and  $I(2\Omega_1)$ , can be determined in several ways, such as using Fourier analysis or a lock-in

amplifier. Since only one channel is required, a single photomultiplier tube can be utilized.

An example of the  $H_\alpha$  signal from the beam is shown in Fig. 3. The interference filter is set at  $\sim 6620 \text{ \AA}$  to compensate for the large Doppler shift from the beam emission. The signal intensity is estimated to be  $\sim 5 \times 10^{12}$  photons sec-sr-cm<sup>2</sup>. The data shown has been smoothed with a running average over one msec time intervals to eliminate the high frequency modulation from the polarimeter. The lock-in amplifier signal, with a one msec integration time constant, is also shown, which illustrates the polarimeter modulation at the PEM resonant frequency. This is also demonstrated, in Fig. 4, with a 16 msec fast Fourier transform(FFT) of the data. The amplitudes at  $2\Omega_1 = 75.48 \text{ kHz}$  and  $2\Omega_2 = 84.09 \text{ kHz}$ , corresponding to the resonant frequencies of the two PEM's, are proportional to the sine and cosine, respectively, of the pitch angle. As illustrated in Fig. 4(b) the uncertainty in the amplitude of the sine component is 1.6 units. This corresponds to  $\sim 0.3^\circ$  for the 16 msec interval. This uncertainty has also been determined from a statistical analysis of the pitch angle variation from many successive discharges.

As discussed earlier in the text, in order to obtain a radial profile to determine  $q(0)$ , a shot-to-shot scan is required. This was done for an Ohmic discharge with a plasma current of 330 kA, major radius of 1.64 m, minor radius of 0.3 m, density of  $3 \times 10^{23} \text{ cm}^{-3}$ , and toroidal field of 1.2 T. Only discharges with the plasma current within 5% of 330 kA were used in the analysis to minimize shot-to-shot variations. The radial scan of the pitch angle is shown in Fig. 5. Each data point in the figure is a time average of 40 msec from three discharges. This reduces the uncertainty to  $0.1^\circ$ , corresponding to  $\sim 20$  Gauss. The safety factor at the magnetic axis, using the



central 7 points from the graph for the linear regression, is  $q_{cyl} = 0.63 \pm 0.02$  assuming a circular plasma. Systematic errors due to the beam viewing geometry amount to an absolute error of  $\sim \pm 2$  cm. Also the zero reference angle of the toroidal field with respect to the polarimeter axis, which is measured with beam injection into a gas-filled torus, introduces some error. However, both these errors cause a shift of the data and do not contribute to the uncertainty in  $q_{cyl}$ . Systematic errors that do contribute to the  $q_{cyl}$  uncertainty include the relative beam viewing geometry error, and vertical displacement from the midplane of the plasma or the field of view. The contribution of these errors increases the uncertainty so that  $q_{cyl} = 0.63 \pm 0.03$ , which illustrates the high precision obtainable with MSE polarimetry. For a noncircular, low beta plasma, such as those described here,  $q(0) = \kappa q_{cyl}$ , where  $\kappa$  is the elongation of a plasma with an elliptical cross section. This correction factor can be derived using the definition for  $q(r)$  and the solution of the Grad-Shafranov equation for a noncircular cross section.<sup>10</sup> Based on results from an equilibrium code and measurements from an X-ray pinhole camera,  $\kappa = 1.36$ , which results in  $q(0) = 0.86 \pm .05$ .

Independent confirmation of this value of  $q(0)$  derived from the MSE polarimetry measurements has been obtained from two other  $q(0)$  measurements on PBX-M for the same set of discharges. One technique uses an X-ray pinhole camera, which can obtain an image of the plasma and determine the shape of the magnetic flux surfaces in the plasma core.<sup>11</sup> The derived poloidal emissivity contours are compared with the poloidal flux contours calculated via a magnetics equilibrium code. An assumed parameterization of the internal current distribution is adjusted, along with  $q(0)$ , to match the measured shape to determine the internal current distribution and  $q(0)$ . The measured electron pressure profiles and several external flux values are used to

constrain the allowed equilibria. This measurement technique is sufficient to constrain the allowed value of the axial safety factor to  $q(0) = 0.7 \pm 0.2$ .

The Fast Ion Diagnostic Experiment (FIDE) is another technique for measuring plasma current profiles, and it has been demonstrated in two previous tokamak experiments.<sup>12,13</sup> A  $q(0)$  of  $0.8 \pm 0.14$ , which represents an average over a sawtooth period, was obtained at 300 msec after the start of the discharge, and is in good agreement with the value from the MSE polarimetry diagnostic.

In conclusion, we have definitive measurements that motional Stark effect polarimetry can yield accurate pitch angle profiles. The result that  $q(0) < 1$  for discharges exhibiting sawtooth behavior is consistent with measurements obtained elsewhere.<sup>4,14</sup> Expected improvements in the design of the diagnostic and the neutral beam will yield an improved signal-to-noise ratio and time resolution. The technique also has the potential for multichannel capability to obtain  $j(r, t)$  profile evolution during a single discharge. Data with this system have also been obtained in beam heated discharges with  $\bar{n}_e = 6 \times 10^{13} \text{ cm}^{-3}$ , indicating this approach extrapolates favorably for use at higher densities and/or in larger machines.

The authors wish to thank M. Okabayashi and the PBX-M group for operation of the tokamak. This work was supported by the U. S. Dept. of Energy under Contract Nos. DE-AC03-86ER80409 and DE-AC02-76-CHO-3073.

## References

- <sup>1</sup>F. DeMarco and S. E. Segre. *Plasma Phys.* **14**, 246 (1972).
- <sup>2</sup>D. Wyóblewski, L. K. Huang, and H. W. Mos. *Phys. Rev. Lett.* **61**, 1724 (1988).
- <sup>3</sup>K. McCormick et al., *Phys. Rev. Lett.* **58**, 491 (1987).
- <sup>4</sup>W. P. West, D. M. Thomas, J. S. DeGrassie, and S. B. Zheng. *Phys. Rev. Lett.* **58**, 2758 (1987).
- <sup>5</sup>E. U. Condon and G. H. Shortley. *The Theory of Atomic Spectra*. Cambridge University Press, 1963.
- <sup>6</sup>M. Okabayashi et al., "Initial Results of the PBX-M Experiment", in *Plasma Physics and Controlled Nuclear Fusion Research, 1988*. IAEA, Vienna (to be published).
- <sup>7</sup>H. W. Kugel et al., *Nucl. Instrum. Methods* (to be published).
- <sup>8</sup>J. C. Kemp, *J. Opt. Soc. Am.* **59**, 950 (1969).
- <sup>9</sup>J. C. Kemp, G. D. Henson, C. T. Steiner, and E. R. Powell. *Nature* **326**, 270 (1987).
- <sup>10</sup>J. P. Freidberg, *Ideal Magnetohydrodynamics*. Plenum Press, New York, 1987.
- <sup>11</sup>R. J. Fonck et al., *Rev. Sci. Instrum.* **59**, 1831 (1988).
- <sup>12</sup>R. J. Goldston, *Phys. Fluids* **21**, 2346 (1978).
- <sup>13</sup>D. D. Meyerhofer et al., *Nucl. Fusion* **25**, 321 (1985).
- <sup>14</sup>H. Soltwisch, *Rev. Sci. Instrum.* **59**, 1599 (1988).

## List of Figures

1. The Stark effect pattern of the Balmer alpha ( $H_\alpha$ ) transition is shown by the vertical lines. The data points are from a spectral scan of the fractional polarization and the solid curve is numerically calculated.
2. Experimental setup of the diagnostic neutral beam and polarimeter on PBX-M.
3. a) PMT and b) lock-in amplifier signal from the neutral beam.
4. FFT analysis at (a)  $2\Omega_1$  which is proportional to  $\cos(2\gamma_p)$  and (b)  $2\Omega_2$  which is proportional to  $\sin(2\gamma_p)$ .
5. Radial scan of the pitch angle.

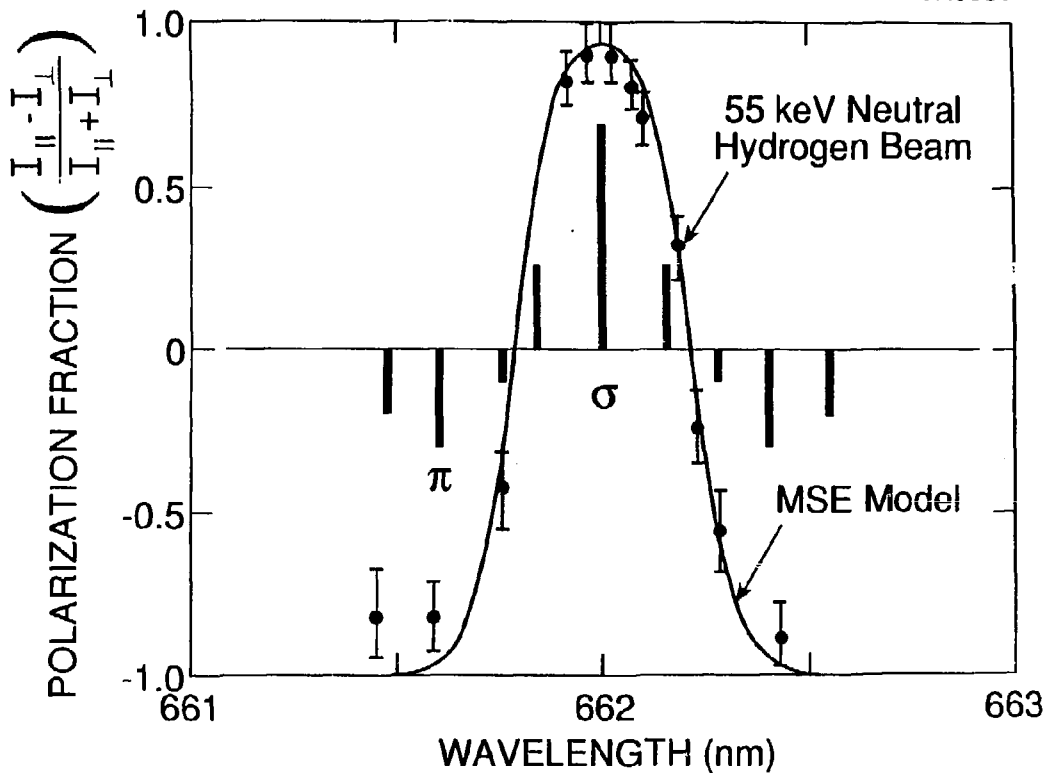


Fig. 1

#89X0053

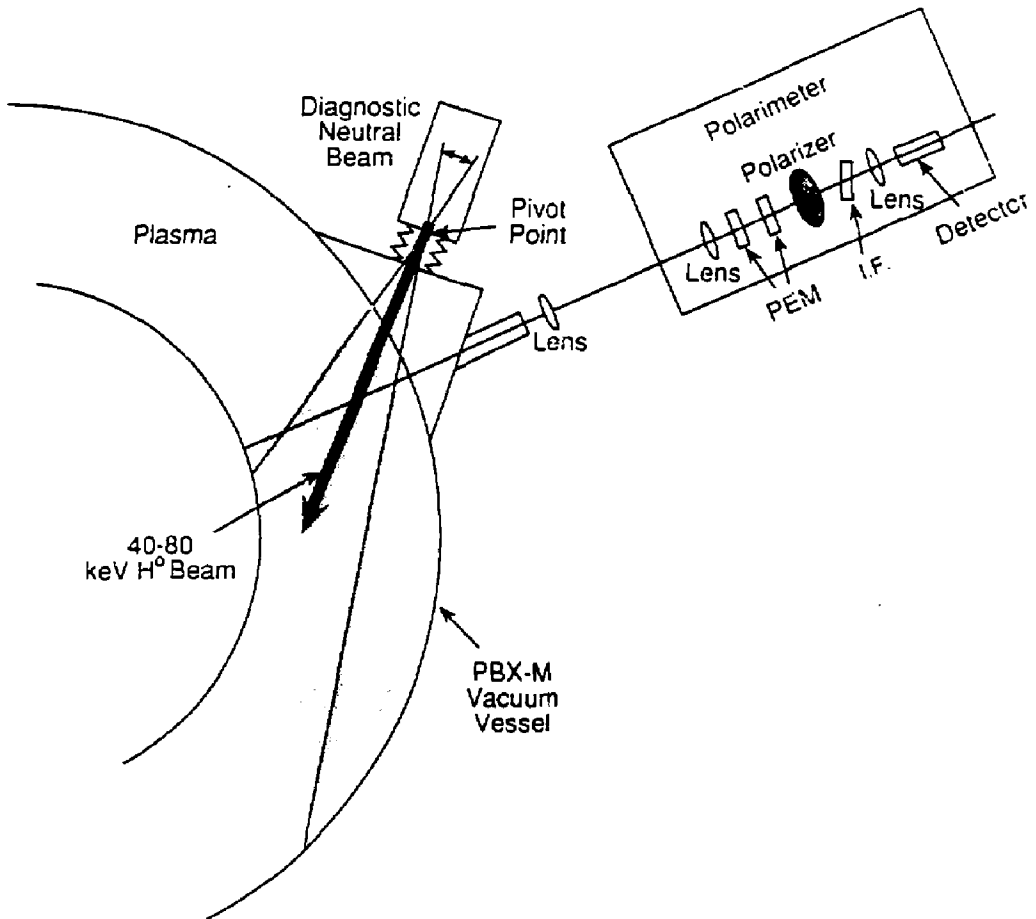


Fig. 2

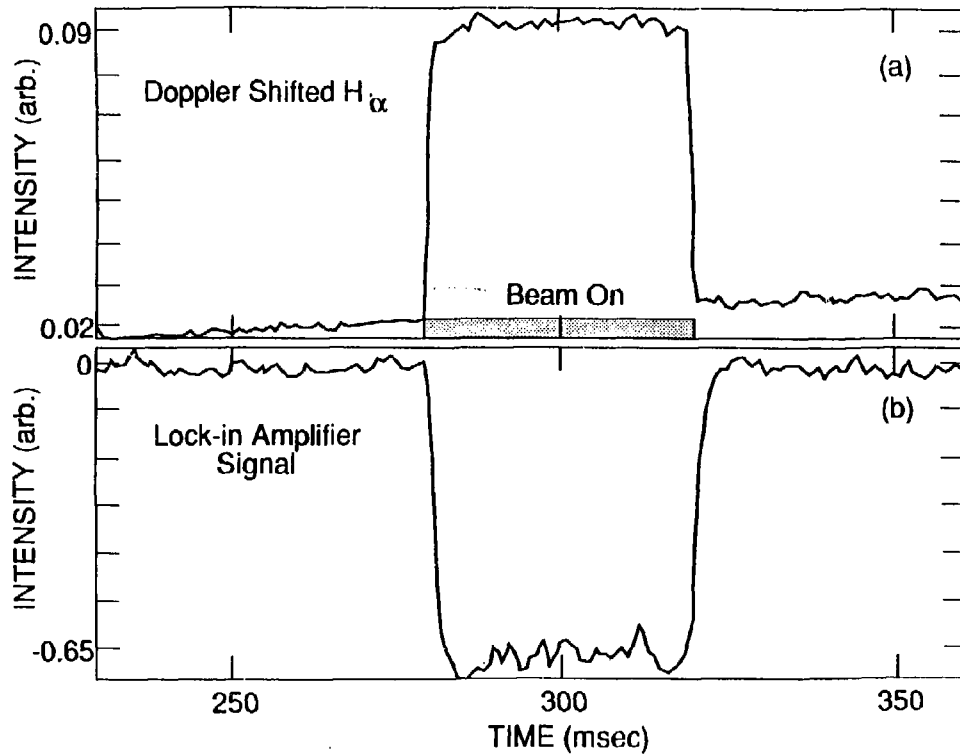


Fig. 3

#89X0055

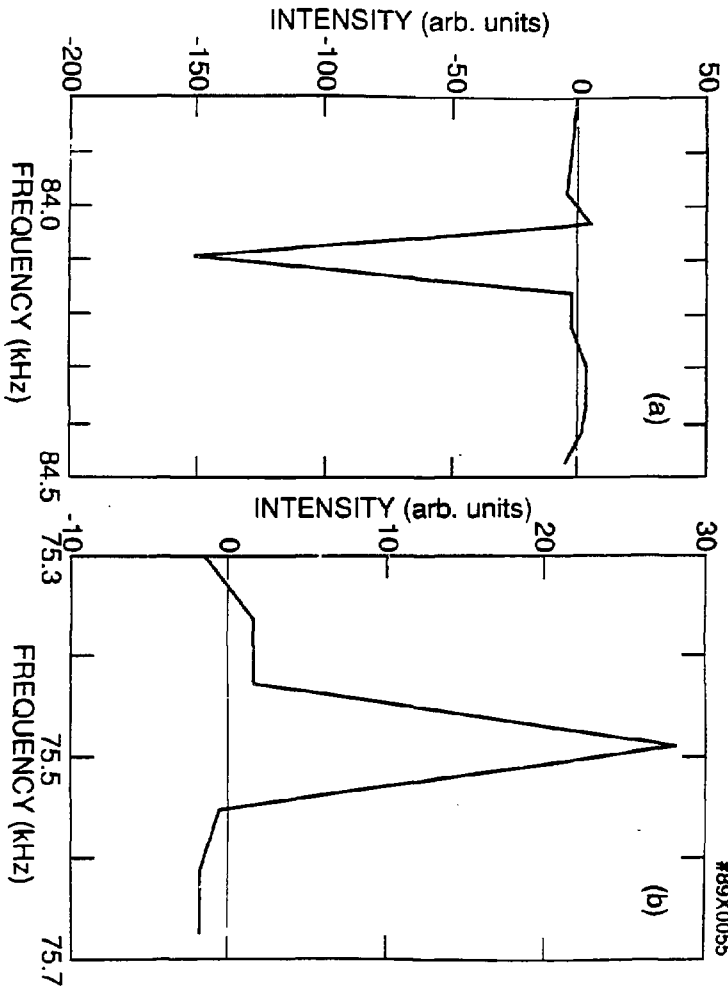


Fig. 4



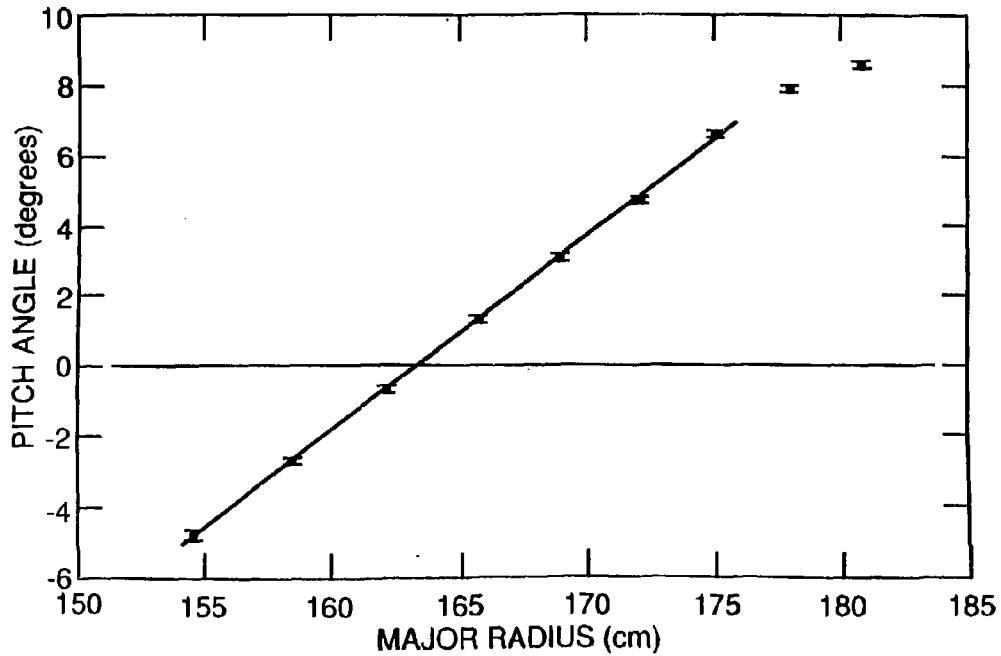


Fig. 5

EXTERNAL DISTRIBUTION IN ADDITION TO UC-420

Dr. Frank J. Paoloni, Univ of Wollongong, AUSTRALIA  
Prof. M.H. Brennan, Univ Sydney, AUSTRALIA  
Plasma Research Lab., Australian Nat. Univ., AUSTRALIA  
Prof. I.R. Jones, Flinders Univ., AUSTRALIA  
Prof. F. Cap, Inst Theo Phys, AUSTRIA  
Prof. M. Heindler, Institut für Theoretische Physik, AUSTRIA  
M. Gossens, Astronomisch Instituut, BELGIUM  
Ecole Royale Militaire, Lab de Phys Plasmas, BELGIUM  
Commission-European, Dg-XII Fusion Prog, BELGIUM  
Prof. R. Boucique, Rijksuniversiteit Gent, BELGIUM  
Dr. P.H. Sakanaka, Instituto Fisica, BRAZIL  
Instituto De Pesquisas Espaciais-INPE, BRAZIL  
Documents Office, Atomic Energy of Canada Limited, CANADA  
Dr. M.P. Bachynski, MPB Technologies, Inc., CANADA  
Dr. H.M. Skarsgård, University of Saskatchewan, CANADA  
Dr. H. Barnard, University of British Columbia, CANADA  
Prof. J. Teichmann, Univ. of Montreal, CANADA  
Prof. S.R. Sreedivasan, University of Calgary, CANADA  
Prof. Tudor W. Johnston, INRS-Energie, CANADA  
Dr. Bolton, Centre canadien de fusion magnetique, CANADA  
Dr. C.R. James, Univ. of Alberta, CANADA  
Dr. Peter Lukac, Komenského Univ, CZECHOSLOVAKIA  
The Librarian, Culham Laboratory, ENGLAND  
The Librarian, Rutherford Appleton Laboratory, ENGLAND  
Mrs. S.A. Hutchinson, JET Library, ENGLAND  
C. Mouttat, Lab. de Physique des Milieux Ionises, FRANCE  
J. Rader, CEN/CADARACHE - Bat 506, FRANCE  
Ms. C. Rinni, Librarian, Univ. of Ioannina, GREECE  
Dr. Tom Mial, Academy Bibliographic Ser., HONG KONG  
Preprint Library, Hungarian Academy of Sciences, HUNGARY  
Dr. B. Das Gupta, Saha Inst of Nucl. Phys., INDIA  
Dr. P. Kaw, Institute for Plasma Research, INDIA  
Dr. Philip Rosenau, Israel Inst. of Tech, ISRAEL  
Librarian, Int'l Ctr Theo Phys, ITALY  
Prof. G. Rostagni, Istituto Gas Ionizzati Del CNR, ITALY  
Miss Clelia De Palo, Assoc EURATOM-ENEA, ITALY  
Dr. G. Grosso, Istituto di Fisica del Plasma, ITALY  
Dr. H. Yamato, Toshiba Res & Dev, JAPAN  
Prof. I. Kawakami, Atomic Energy Res. Institute, JAPAN  
Prof. Kyoji Nishikawa, Univ of Hiroshima, JAPAN  
Director, Dept. Large Tokamak Res. JAERI, JAPAN  
Prof. Satoshi Itoh, Kyushu University, JAPAN  
Research Info Center, Nagoya University, JAPAN  
Prof. S. Tanaka, Kyoto University, JAPAN  
Library, Kyoto University, JAPAN  
Prof. Nobuyuki Inoue, University of Tokyo, JAPAN  
S. Mori, JAERI, JAPAN  
H. Jeong, Librarian, Korea Advanced Energy Res Inst, KOREA  
Prof. D.I. Choi, The Korea Adv. Inst of Sci & Tech, KOREA  
Prof. B.S. Liley, University of Waikato, NEW ZEALAND  
Institute of Plasma Physics, PEOPLE'S REPUBLIC OF CHINA  
Librarian, Institute of Phys., PEOPLE'S REPUBLIC OF CHINA  
Library, Tsing Hua University, PEOPLE'S REPUBLIC OF CHINA  
Z. Li, Southwest Inst. Physics, PEOPLE'S REPUBLIC OF CHINA  
Prof. J.A.C. Cabral, Inst Superior Tecnico, PORTUGAL  
Dr. Octavian Petrus, AL I CUZA University, ROMANIA  
Dr. Jam de Villiers, Fusion Studies, AEC, SO AFRICA  
Prof. M.A. Hellberg, University of Natal, SO AFRICA  
C.I.E.M.A.T., Fusion Div. Library, SPAIN  
Dr. Lennart Stenflo, University of UMEA, SWEDEN  
Library, Royal Institute of Tech, SWEDEN  
Prof. Hans Wilhelmson, Chalmers Univ of Tech, SWEDEN  
Centre Phys des Plasmas, Ecole Polytech Fed, SWITZERLAND  
Bibliotheek, Fom-Inst Voor Plasma-Fysica, THE NETHERLANDS  
Metin Durgut, Middle East Technical University, TURKEY  
Dr. D.D. Ryutov, Siberian Acad Sci, USSR  
Dr. G.A. Eliseev, Kurchatov Institute, USSR  
Dr. V.A. Glukhikh, Inst Electrophysical Apparatus, USSR  
Prof. O.S. Padichenko, Inst. of Phys. & Tech. USSR  
Dr. L.M. Kovrizhnykh, Institute of Gen. Physics, USSR  
Nuclear Res. Establishment, Julich Ltd., W. GERMANY  
Bibliothek, Inst. Fur Plasmaforschung, W. GERMANY  
Dr. K. Schindler, Ruhr-Universität Bochum, W. GERMANY  
ASDEX Reading Rm, c/o Wagner, IPP/Max-Planck, W. GERMANY  
Librarian, Max-Planck Institut, W. GERMANY  
Prof. R.K. Janev, Inst of Phys, YUGOSLAVIA